

Reduced glutathione ameliorates acute kidney injury by inhibiting ferroptosis

LEYU HE and YUAN SHI

Department of Nephrology, Jiaxing Second Hospital, Jiaxing, Zhejiang 314000, P.R. China

Received November 3, 2022; Accepted April 3, 2023

DOI: 10.3892/mmr.2023.13011

Abstract. Reduced glutathione (RGS) can participate in the redox process in the body and inhibit damage to important organs caused by free radicals. Due to its broad biological effects, in addition to its clinical applications in treatment of liver diseases, RGS is also used in the treatment of numerous other diseases, such as malignant tumors and nerve, urological and digestion diseases. However, there are few reports of RGS being used in treatment of acute kidney injury (AKI), and the mechanism of its action in AKI is not clear. To assess the possible mechanism of RGS inhibition in AKI, a mouse AKI model and HK-2 cell ferroptosis model were built to perform *in vitro* and *in vivo* experiments. The levels of blood urea nitrogen (BUN) and malondialdehyde (MDA) before and after the RGS treatment were assessed, and the pathological changes of the kidneys were assessed using hematoxylin and eosin staining. Immunohistochemical (IHC) methods were used to evaluate the expressions of acyl-CoA synthetase long-chain family member 4 (ACSL4) and glutathione peroxidase (GPX4) in the kidney tissues, reverse transcription-quantitative PCR and western blotting were used to assess the levels of ferroptosis marker factors in the kidney tissues and HK-2 cells, and flow cytometry was used to assess cell death. The results indicated that, RGS intervention reduced the BUN and serum MDA levels, and ameliorated glomerular damage and the level of renal structure damage in the mouse model. IHC results demonstrated that RGS intervention could significantly reduce the ACSL4 mRNA expression level and inhibit iron accumulation, and significantly upregulate the GPX4 mRNA expression level. Moreover, RGS could inhibit ferroptosis induced by ferroptosis inducers erastin and RSL3 in HK-2 cells. Cell assay results demonstrated that RGS could improve the lipid oxide level and cell viability, and inhibit cell death, so as to ameliorate the effects of AKI. These results suggested that RGS could ameliorate AKI by

inhibiting ferroptosis, which indicates RGS as a promising therapeutic strategy for the treatment of AKI.

Introduction

Acute kidney injury (AKI) is a common clinical phenomenon, and a major cause of high morbidity and mortality during the perioperative period (1-3). During the short term (~6 h) after AKI has occurred, the glomerular filtration decreases sharply, the serum creatinine and blood urea nitrogen (BUN) increase, and the urine volume decreases, which results in variable kidney damage and eventually chronic kidney disease or terminal-stage renal disease (4,5). Conservative treatment and renal alternative therapy are the commonly used treatments for AKI; however, they cannot effectively prevent or intervene in AKI. Therefore, there is an urgent need to for research on the pathogenesis of AKI and the development of new treatment options, so as to improve the treatment effects of AKI.

Ferroptosis is an iron-dependent non-apoptotic type of cell death caused by intracellular lipid peroxidation metabolism disorder, which is mainly characterized by the accumulation of lipid peroxides and the overload of iron ions (6). When the acyl-CoA synthetase long-chain family member 4 (ACSL4) is overactivated and the glutathione peroxidase (GPX4) expression is reduced, iron accumulates and induces ferroptosis (7). It has been reported that ferroptosis is also a major pathological basis for the occurrence and development of AKI (8).

Reduced glutathione (RGS) combines with peroxides and free radicals, which provides anti-oxidation effects, regulates the metabolism and protects cells. RGS has been used in the adjuvant therapy of numerous diseases, such as liver, brain and kidney diseases. It has been previously reported that RGS can provide protective effects in ischemia-reperfusion AKI (9), but whether its protective mechanism is related to ferroptosis is unclear.

In the present study, by constructing *in vitro* and *in vivo* AKI models, with ferroptosis as an entry point, the mechanism of RGS in ameliorating AKI was evaluated.

Materials and methods

HK-2 cell culture. HK-2 cells were purchased from The Cell Bank of Type Culture Collection of The Chinese Academy of Sciences, and cultured in DMEM (containing 10% fetal bovine serum, 100 U/ml penicillin and 100 U/ml streptomycin; Gibco;

Correspondence to: Dr Leyu He, Department of Nephrology, Jiaxing Second Hospital, 1518 Huancheng Road North, Jiaxing, Zhejiang 314000, P.R. China
E-mail: leyu_he@sina.com

Key words: acute kidney injury, ferroptosis, reduced glutathione

Thermo Fisher Scientific, Inc.) at 37°C in a 5% CO₂ incubator. When the cells were cultured to 90% confluency, they were treated using 0.25% trypsin for 2-3 min at 37°C and seeded on a 6-well plate at a density of 1x10⁵/well. After overnight culture in the aforementioned conditions, cells were grouped and treated to generate the HK-2 cell ferroptosis model and intervention as follows: i) Control group; ii) erastin (ferroptosis inducer) group (10 μmol/l erastin); iii) RSL3 (ferroptosis inducer) group (0.1 μmol/l RSL3) (10); iv) erastin + RGSB group (10 μmol/l erastin for 24 h then 10 mmol/l RGSB was added); and v) RSL3 + RGSB group (0.1 μmol/l RSL3 for 24 h then 10 mmol/l RGSB was added) (11).

Mouse AKI model. The animal use plan was approved by the Animal Care and Use Committee of Jiaying Second Hospital (approval no. 20200713-2). The specific pathogen free BALB/c mice (n=30) were purchased from Beijing Vital River Laboratory Animal Technology Co., Ltd. Same sex litter mates were housed together in individually ventilated cages with two or four mice/cage. During the whole duration of the experiment (7 days), all mice were maintained on a regular diurnal 12 h light/dark cycle with *ad libitum* access to food and water. The study was performed strictly according to The Guide for Care and Use of Laboratory Animals formulated by National Institutes of Health. The researchers monitored animals twice daily. Health was monitored by weight (twice weekly), food and water intake, and general assessment of animal activity. Humane endpoints to help minimize harm, complied with the humane standards of the American Veterinary Medical Association (12), including the mice showed an inability to feed and drink on their own, weight loss of >20% of their starting body weight, were clearly depressed in the absence of anesthesia, did not respond to shouts of repulsion, were unable to move freely, or their body temperature was consistently below 37°C. A total of eighteen mice (male; age, 6-8 weeks) were randomly divided into the control group, model group and RGSB group (n=6).

Anesthesia was administered intraperitoneally using sodium pentobarbital (50 mg/kg). The depth of anesthesia was assessed for ~5 min and mice were placed immediately on a 37°C thermostatic heating pad. After the mice were anesthetized, an incision of 1.5-2.0 cm was cut along the midline of the abdomen, and the skin and peritoneum were separated layer by layer. After entering the abdominal cavity, the left and right renal pedicles were quickly blocked using non-invasive micro-arterial clips. A change in the color of the kidneys from bright red to purple-black, indicated that clipping was successful. After 45 min of clipping, the arterial clip was removed, and blood perfusion was restored. At this point, the kidneys quickly changed from purple-black to bright red, returning to their original color. After the operation, the abdominal cavity was closed by layered suture. The overall duration of the experiment was limited to 60 min. A total of 1 h after successful modeling, the mice in the RGSB group received an intraperitoneal injection of 800 mg/kg RGSB (13) and the mice in the other two groups were administered an equal volume of normal saline, this was repeated for 6 consecutive days. After the operation, the mice were kept warm at 24-29°C, and provided with water and feed. At the end of the experimental period, the mice were anesthetized using

50 mg/kg sodium pentobarbital, and the orbital blood was collected and stored at 4°C overnight. Mice were euthanized by cervical dislocation and death was verified by absence of heartbeat and pupil dilation. The kidneys were collected after euthanasia and after stripping off the capsule, part of the tissues were fixed using 10% formalin at 45°C for 1 h and embedded in paraffin. RNA and protein were extracted from the remaining tissues.

Detection of BUN and malondialdehyde (MDA) levels. The collected blood was centrifuged at 1,006 x g for 10 min at room temperature, and then, the serum was transferred into a new Eppendorf tube. The MDA and BUN levels were quantified using the BUN Detection research-use-only kit (cat. no. EIABUNX10; Invitrogen; Thermo Fisher Scientific, Inc.) and MDA Assay Kit (competitive ELISA) (cat. no. ab238537; Abcam) according to the manufacturers protocols.

Staining and immunohistochemistry (IHC). The fixed, paraffin embedded kidney tissues were cut into 5 μm thick sections. After baking (68°C), the slices were dewaxed with xylene and rehydrated with ethanol in a descending alcohol series. Then, hematoxylin and eosin (H&E) staining and Prussian blue staining were performed according to the manufacturer's protocol, an optical microscope (Nikon Corporation) was used for observation and imaging, and ImageJ 2.0.0 (National Institutes of Health) was used for analysis.

The protein expression levels of ACSL4 and GPX4 in the kidney were assessed using immunohistochemistry. After dewaxing, rehydration and antigen retrieval according to the aforementioned method, the sample was endogenous peroxidase activity was quenched using 3% hydrogen peroxide solution and the sections were blocked using 5% bovine serum albumin (Roche Diagnostics GmbH) for 10 min at room temperature. Sections were incubated with primary antibodies against ACSL4 (1:200; cat. no. PA5-30026; Invitrogen; Thermo Fisher Scientific, Inc.) and GPX4 (1:200; cat. no. PA5-10251; Invitrogen; Thermo Fisher Scientific, Inc.) overnight at 4°C. The sections were then washed with PBS, and incubated with Goat anti-Rabbit IgG (H+L) Secondary Antibody (cat. no. 31210; Invitrogen; Thermo Fisher Scientific, Inc.) for 1 h at room temperature. After washing the sample, DAB color development was performed for 45 s. Sections were imaged using an optical microscope (Nikon Corporation) with a x400 objective, and the cells with positive staining were quantified using ImageJ 2.0.0 (National Institutes of Health).

Reverse transcription-quantitative PCR (RT-qPCR). Total RNA was extracted from the mouse kidney and HK-2 cells using a column-type animal tissue total RNA extraction and purification kit (Sangon Biotech Co., Ltd.), and then reverse transcribed to synthesize complementary DNA using a PrimeScript™ RT Reagent Kit with gDNA Eraser Kit (Takara Bio, Inc.). qPCR was performed using the TB Green® Premix Ex Taq™ II Kit (Takara Bio, Inc.), with GAPDH as the control gene. The thermal program included the following melting curve steps: 10 min at 95°C for 1 cycle, followed by 40 cycles for 10 sec at 95°C, 20 sec at 60°C and 15 sec at 72°C, and then a gradual increase from 72°C to 95°C at 0.5°C per sec; the data were collected every 6 sec. Changes in the mRNA

Table I. Sequences of the primers used for reverse transcription-quantitative PCR.

Gene	Sequence (5'-3')
m-GPX4	F: GTGGAAATGGATGAAAGTC R: AGCCGTTCTTATCAATGA
h-GPX4	F: TGTGGAAGTGGATGAAGA R: ATGAGGAAGTGTGGAGAG
m-ACSL4	F: CTTCCTCTTAAGGCCGGGAC R: TGCCATAGCGTTTTTCTTAGATTT
h-ACSL4	F: AAGTGAATCGCAGAGTGAATA R: AGAAGATGGCAATGGTGTT
m-GAPDH	F: TGTGTCCGTCGTGGATCTGA R: TTGCTGTTGAAGTCGCAGGAG
h-GAPDH	F: GAAGGCTGGGGCTCATT R: CAGGAGGCATTGCTGATGAT

ACSL4, acyl-CoA synthetase long-chain family member 4; GPX4, glutathione peroxidase; m, mouse; h, human.

expression levels were calculated using the $2^{-\Delta\Delta C_q}$ method (14). All experiments were performed according to the manufacturer's protocols, and the primer sequences used were presented in Table I.

Western blotting. Total protein from the kidneys and HK-2 cells in each group collected using RIPA buffer (Thermo Fisher Scientific, Inc.), and the protein content was determined using the BCA method. SDS-PAGE gel electrophoresis was performed, equal amounts of protein (40 μ g) were separated on 10% gels using SDS-PAGE and the samples were then transferred to polyvinylidene fluoride membranes. The membranes were blocked with 3% skimmed milk at room temperature for 1 h, and incubated with primary antibodies against ACSL4 (1:1,000; cat. no. PA5-30026), GPX4 (1:1,000; cat. no. PA5-10251) and GAPDH (1:5,000; cat. no. MA1-16757) (all Invitrogen; Thermo Fisher Scientific, Inc.) overnight at 4°C. Membranes were washed using TBST [50 mmol/l Tris-HCl (pH 8.0), 150 mmol/l NaCl, and 0.1% Tween-20] then incubated with HRP-conjugated goat anti-rabbit IgG (H+L) secondary antibodies (1:2,000; cat. no. 31460; Invitrogen; Thermo Fisher Scientific, Inc.) at room temperature for 1 h. Finally, the color was developed using ECL supersensitive luminescent solution (Thermo Fisher Scientific, Inc.), and images were collected and analyzed using a Bio-Rad Gel Doc XR+ imaging system (Bio-Rad Laboratories, Inc.).

Cell viability assay. HK-2 cells were seeded in the 96-well plate at a density of 1.5×10^3 cells/well. After 48 h of culture (at 37°C in a 5% CO₂ incubator), the CCK-8 working solution was added to the sample and incubated for 1 h. The absorbance of the cells in the wells was then measured at 490 nm using the Multiskan Sky Microplate Spectrophotometer (Thermo Fisher Scientific, Inc.) to evaluate the cell viability.

Detection of apoptosis by flow cytometry. HK-2 cells were seeded into a 6-well plate and the number of cells was adjusted

to $\sim 1 \times 10^5$ after trypsinization. Samples were then centrifuged at 200 x g at room temperature for 5 min, the supernatant was discarded, and the cells were resuspended in PBS. A total of 5 μ l of Annexin V-FITC and 5 μ l of propidium iodide were added to each well, were mixed by pipetting, and incubated at room temperature in the dark for 15 min. The samples were then assessed using MACSQuant Analyzer 16 (Miltenyi Biotec GmbH) and data analyses were processed using FlowJo v10.6.2 software (FlowJo, LLC).

Statistical methods. The statistical analysis was conducted using GraphPad Prism 9 (Graphpad Software; Dotmatics). All data are presented as the mean \pm standard deviation. Differences between groups were statistically analyzed using one-way analysis of variance and Tukey's post-hoc test. $P < 0.05$ was considered to indicate a statistically significant difference.

Results

RGSH can inhibit ferroptosis in mice with AKI. The H&E staining results of the renal tubular epithelial cells in the mice in the AKI model group demonstrated massive atrophy and necrosis, the tubular space was widened, and the kidney structure was severely damaged. The glomerular damage in mice in the RGSH group was alleviated and the level of renal structural damage was reduced. The IHC results demonstrated that ACSL4 protein expression levels increased markedly, and GPX4 protein expression levels decreased markedly in the AKI model group compared with the control group. However, the ACSL4 protein expression levels were markedly decreased and the GPX4 protein expression levels were markedly increased in the RGSH group compared with the AKI model group (Fig. 1A and B). The BUN and MDA levels of mice in different groups was assessed. Compared with the control group, the BUN and MDA levels in the AKI model group were markedly increased, whereas the BUN and MDA levels in the RGSH group were markedly lower than that of the AKI model group, which indicated recovery (Fig. 1C). The level of iron ions in the glomerulus of mice in the model group was significantly higher than that in the control group, whereas the iron ion level in the RGSH group was significantly lower than that in the AKI model group. (Fig. 1D). The mRNA expression levels of ACSL4 and GPX4, assessed using RT-qPCR were consistent with the IHC results. The mRNA expression level of ACSL4 increased significantly and the mRNA expression level of GPX4 decreased significantly in the AKI group compared with the control; however, the mRNA expression level of ACSL4 decreased significantly and the mRNA expression level of GPX4 increased significantly in the RGSH group compared with the AKI group (Fig. 1E). These results demonstrated that the acute kidney injury induces ferroptosis in the renal cells and that RGSH ameliorated this process.

RGSH can inhibit ferroptosis induced by ferroptosis inducers erastin and RSL3 in HK-2 cells. A HK-2 cell ferroptosis model was constructed using erastin and RSL3. The flow cytometry results demonstrated that the RGSH intervention could markedly reduce cell death caused by ferroptosis (Fig. 2A). The statistical comparison of apoptosis rate is shown in Fig. 2B. The results of cell viability experiments

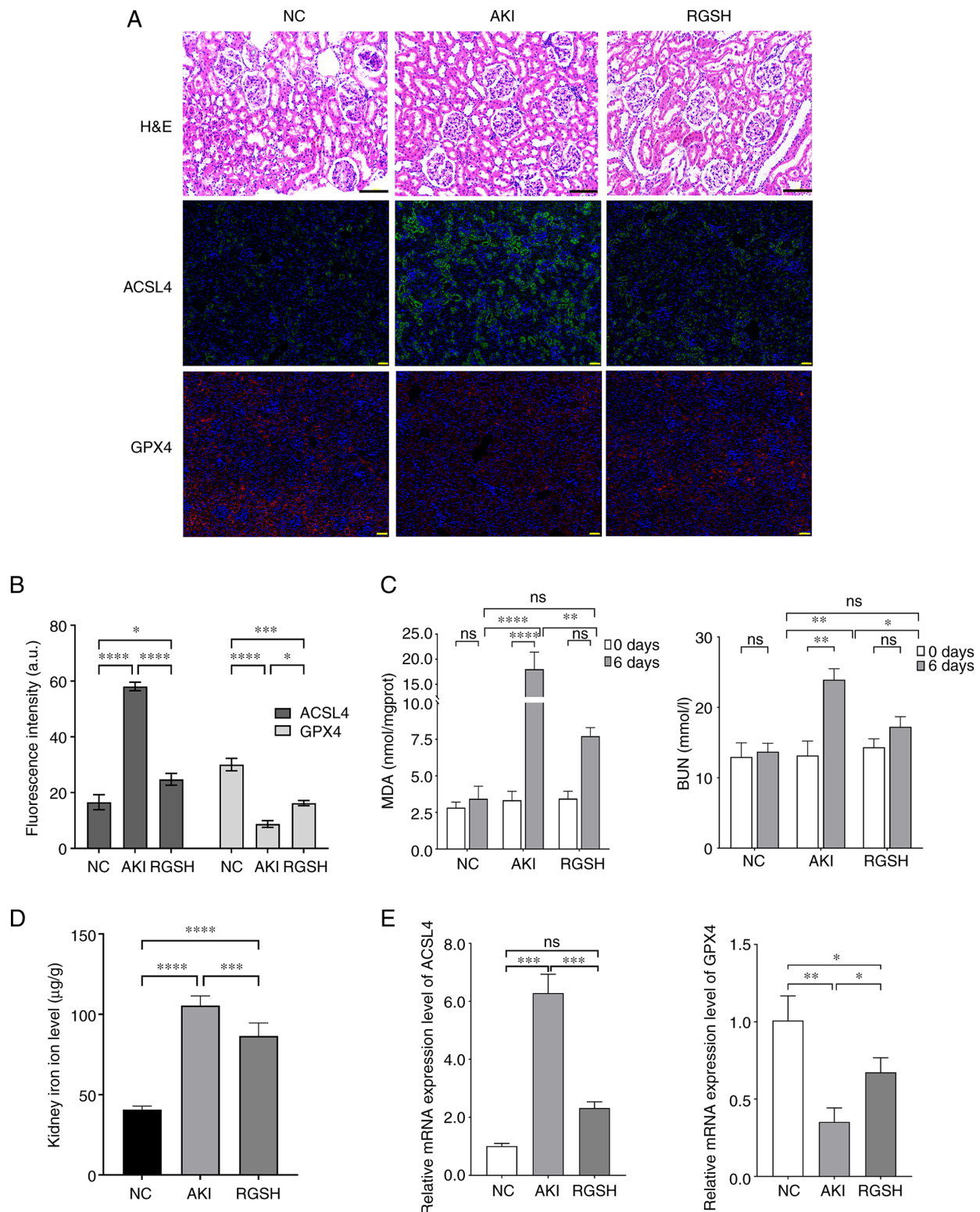


Figure 1. Detection of mouse AKI indexes. (A) Renal injury in the glomeruli of mice in various groups assessed using H&E staining and the protein expression of ACSL4 and GPX4 in the mouse kidney in different groups according assessed using immunohistochemical staining. (B) The fluorescence intensity of ACSL4 or GPX4-expressing region in immunofluorescence (Fig. 1A) was calculated using ImageJ software. (C) BUN and MDA levels of mice in different groups. (D) Iron ion level in the glomeruli of mice in various groups. (E) mRNA expression levels of ACSL4 and GPX4 assessed using reverse transcription-quantitative PCR. Scale bars: H&E, 100 μm ; IHC, 50 μm . * $P < 0.05$, ** $P < 0.01$ and *** $P < 0.001$. AKI, acute kidney injury; ACSL4, acyl-CoA synthetase long-chain family member 4; BUN, blood urea nitrogen; GPX4, glutathione peroxidase; H&E, hematoxylin and eosin; MDA, malondialdehyde; NC, negative control; RGSH, reduced glutathione; ns, not significant.

demonstrated that cell viability in the erastin and RSL3 model groups were significantly reduced compared with the control. After RGSH intervention, the cell viabilities were

significantly enhanced and markedly recovered (Fig. 2C). Furthermore, RGSH intervention also significantly alleviated the reduction in lipid oxide levels caused by ferroptosis

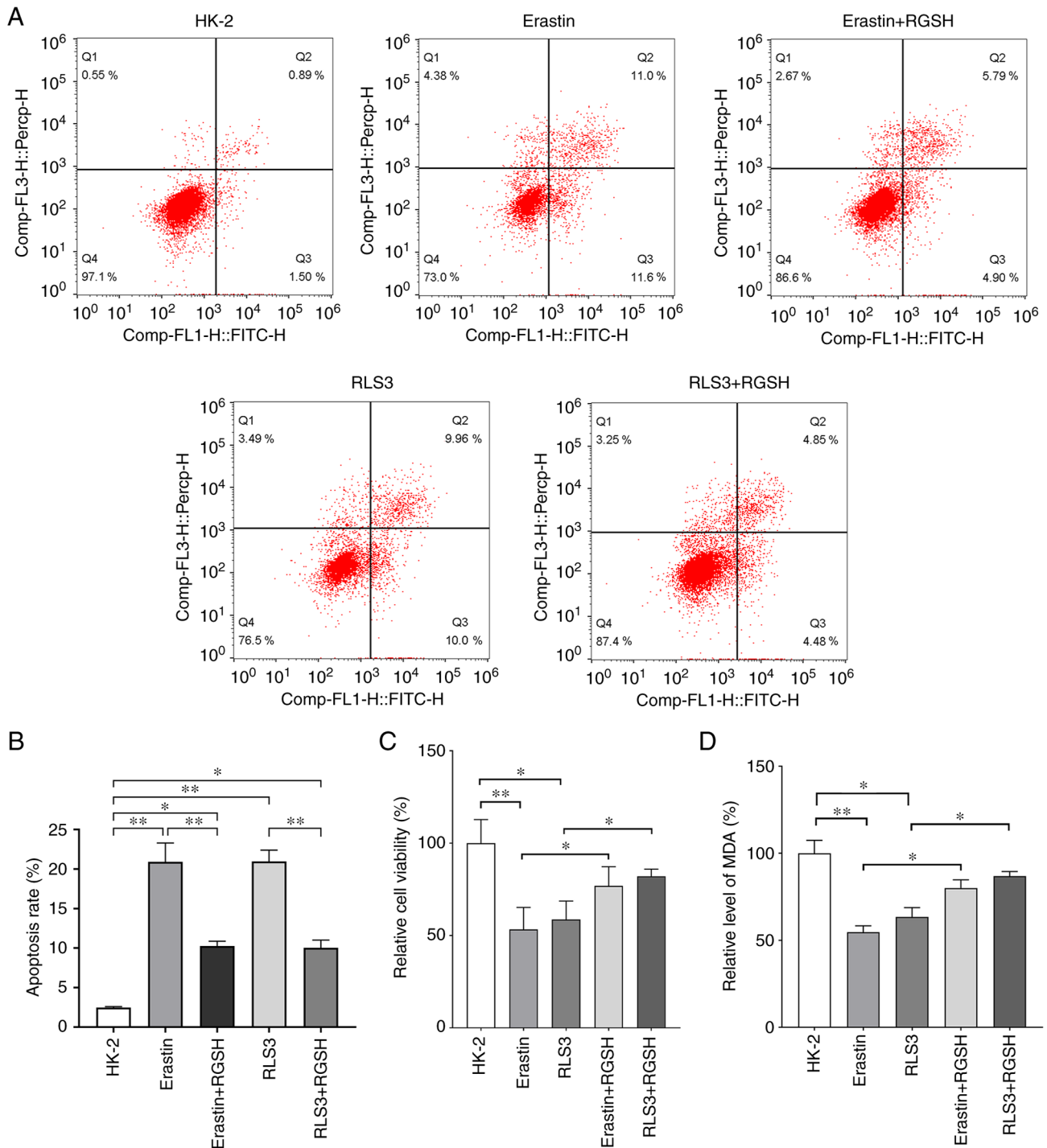


Figure 2. RGSF can alleviate ferroptosis of HK-2 cells. (A) Cell apoptosis of different groups assessed using flow cytometry. (B) The statistical analysis of apoptosis rate. (C) Cell viabilities of different groups assessed using CCK-8 (relative to HK-2). (D) RGSF can improve the level of lipid oxide in cells (relative to HK-2). * $P < 0.05$ and ** $P < 0.01$. RGSF, reduced glutathione; MDA, malondialdehyde.

inducers (Fig. 2D). These results indicated that RGSF could inhibit the ferroptosis of HK-2 cells induced by the ferroptosis inducers erastin and RSL3.

RGSF can inhibit ferroptosis through the regulation of the levels of ferroptosis-related proteins. RT-qPCR was used to assess detect the mRNA expression levels of the ferroptosis-related proteins ACSL4 and GPX4 in HK-2 cells under certain treatments. In the model groups which used erastin and RSL3 to induce ferroptosis, the mRNA expression level

of ACSL4 increased significantly and the mRNA expression level of GPX4 decreased significantly compared with the control. Compared with their respective model groups, in both the erastin + RGSF and RSL3 + RGSF groups, the mRNA expression level of ACSL4 decreased significantly and the mRNA expression level of GPX4 increased significantly (Fig. 3A). The protein expression levels of ACSL4 and GPX4 semi-quantified using western blotting were consistent with the RT-qPCR results (Fig. 3B and C). These results suggested that RGSF intervention could restore the changes

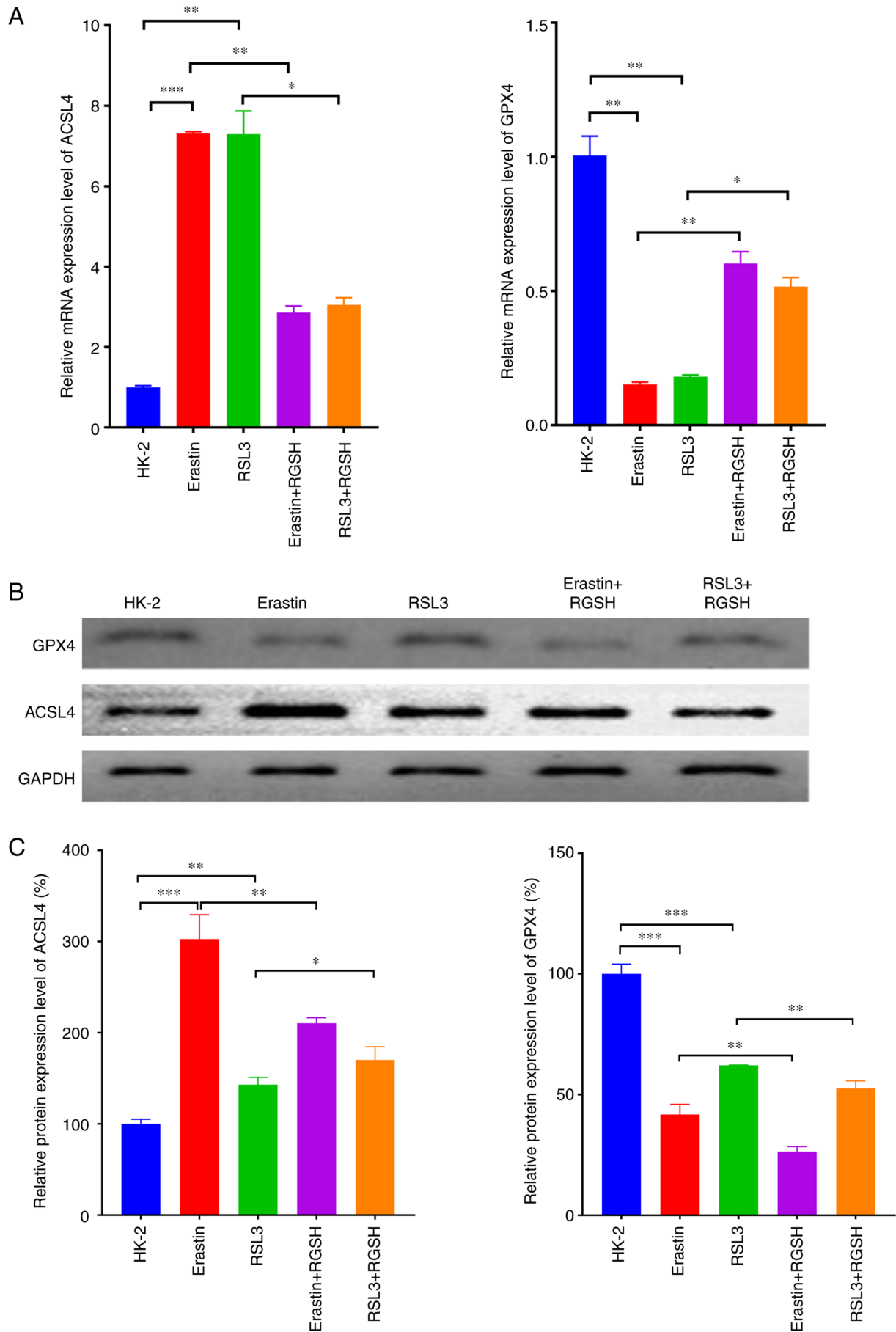


Figure 3. Detection of expression levels of ferroptosis-related proteins. (A) mRNA expression levels of ACSL4 and GPX4 assessed using reverse transcription-quantitative PCR. (B) Western blots of ACSL4 and GPX4 protein expression. (C) Relative protein expression levels of ACSL4 and GPX4. * $P < 0.05$, ** $P < 0.01$ and *** $P < 0.001$. ACSL4, acyl-CoA synthetase long-chain family member 4; GPX4, glutathione peroxidase; RGSH, reduced glutathione.

in ferroptosis-related proteins induced by the ferroptosis inducers, thereby inhibiting ferroptosis.

Discussion

The damage to red blood cells during the perioperative period can cause hemoglobin to escape and enter the kidney through the blood circulation, which can lead to AKI. Different degrees of renal damage affect the quality of life and long-term prognosis of the patients (15,16). When AKI occurs, the renal tubules are damaged and the glomerular filtration rate drops sharply, which results in an increase in serum creatinine and blood urea nitrogen (17). In the AKI mouse model built in present study, the BUN and serum MDA levels markedly increased, marked glomerular damage occurred and it was demonstrated that the RGSH intervention could alleviate these effects, which demonstrated the protective effect of RGSH in AKI.

Ferroptosis is widely present in a number of cells types and regulates numerous pathological processes, including those involved in certain neurodegenerative diseases (such as Alzheimer's disease), tumors, stroke and traumatic brain injury (18-21). Ferroptosis affects the occurrence and development of AKI (8,22). Therefore, attenuation of ferroptosis could be an important strategy to ameliorate AKI. The expression levels of ferroptosis-related factors, including lipid oxides, iron ions, ACSL4 and GPX4, are closely related to the degree of ferroptosis in AKI (23-26). The present study demonstrated that when AKI occurred, the iron ion level in the renal tissues increased significantly, the mRNA expression level of ACSL4 increased significantly and the mRNA expression level of GPX4 decreased significantly, which indicated the occurrence of ferroptosis in the kidney.

Previous studies have reported that RGSH can inhibit oxidative stress and thus alleviate liver damage (27), and improve renal function in patients by reducing the serum creatinine levels (28). A study has also reported that RGSH can effectively eliminate oxygen free radicals and treat the AKI rats with ischemia reperfusion (29). These studies suggested that RGSH served a protective role for the body through its redox function. In the present study, RGSH reduced the level of iron ions and ACSL4 in AKI, and increased the expression of GPX4, thereby reducing the degree of kidney damage, which demonstrated that RGSH could ameliorate hemolytic AKI via regulation of the ferroptosis pathway, which was consistent with the results of previous studies that RGSH affects ferroptosis via regulation of the ferroptosis-related gene GPX4 (30). In the *in vitro* experiments, construction of the HK-2 cell ferroptosis model demonstrated that RGSH could significantly increase cell viability and significantly increase the lipid oxide level in cells, which inhibited cell apoptosis. These results indicated that RGSH may inhibit cell death through the ferroptosis signaling pathway and exert a protective effect on AKI. However, the experiments in the present study were not sufficient to completely elucidate the underlying mechanisms of ferroptosis in AKI through molecular and animal model experiments alone, and similarly RGSH intervention on AKI is only a meaningful first experiment. Although the results of the present study indicated that RGSH could improve the poor outcomes of AKI by modulating the ferroptosis signaling

pathway, the mechanisms underlying the occurrence of ferroptosis in AKI have not been evaluated in depth. We hypothesize that another major cause of AKI is the release of hemoglobin from ruptured erythrocytes following major open surgery (31); however, the use of hemoglobin chloride for stimulating kidney injury does not accurately mimic the features of open surgery. Further study is required to develop the model of surgical AKI, including partial hepatectomy in mice.

In conclusion, RGSH intervention can down-regulate the renal ACSL4 mRNA expression level and up-regulate the GPX4 mRNA expression level in the development of AKI, and reduce the lipid oxide and iron ion levels, thereby reducing iron accumulation, alleviating cell damage and ameliorating intraoperative AKI by inhibiting ferroptosis. The protective effect of RGSH on AKI by inhibiting ferroptosis provides a new therapeutic strategy, which could guide the use of medication and the treatment of perioperative AKI in the clinic.

Acknowledgements

Not applicable.

Funding

No funding was received.

Availability of data and material

The datasets used and/or analyzed during the current study are available from the corresponding author on reasonable request.

Authors' contributions

LH performed the histological examination of the kidney and YS performed the molecular biology experiments. LH wrote the manuscript. LH and YS confirm the authenticity of all the raw data. Both authors read and approved the final manuscript.

Ethics approval and consent to participate

The present study was performed strictly following The Guide for Care and Use of Laboratory Animals formulated by National Institutes of Health. The animal use plan was approved by the Animal Care and Use Committee of Jiaxing Second Hospital (approval no. 20200713-2).

Patient consent for publication

Not applicable.

Competing interests

The authors declare that they have no competing interests.

References

1. Hounkpatin H, Fraser S, Glidewell L, Blakeman T, Lewington A and Roderick P: Predicting risk of recurrent acute kidney injury: A systematic review. *Nephron* 142: 83-90, 2019.
2. Saadat-Gilani K and Zarbock A: Perioperative renal protection. *Curr Opin Crit Care* 27: 676-685, 2021.

3. Calvert S and Shaw A: Perioperative acute kidney injury. *Perioper Med (Lond)* 1: 6, 2012.
4. Singbartl K and Kellum J: AKI in the ICU: Definition, epidemiology, risk stratification, and outcomes. *Kidney Int* 81: 819-825, 2012.
5. Sul YH, Lee JY, Kim SH, Ye JB, Lee JS, Yoon SY and Choi JH: Risk factors for acute kidney injury in critically ill patients with torso injury: A retrospective observational single-center study. *Medicine (Baltimore)* 100: e26723, 2021.
6. Dixon S and Stockwell B: The role of iron and reactive oxygen species in cell death. *Nat Chem Biol* 10: 9-17, 2014.
7. Sha R, Xu Y, Yuan C, Sheng X, Wu Z, Peng J, Wang Y, Lin Y, Zhou L, Xu S, *et al*: Predictive and prognostic impact of ferroptosis-related genes ACSL4 and GPX4 on breast cancer treated with neoadjuvant chemotherapy. *EBioMedicine* 71: 103560, 2021.
8. Carney E: Ferroptotic stress promotes the AKI to CKD transition. *Nat Rev Nephrol* 17: 633, 2021.
9. Park EJ, Dusabimana T, Je J, Jeong K, Yun SP, Kim HJ, Kim H and Park SW: Honokiol protects the kidney from renal ischemia and reperfusion injury by upregulating the glutathione biosynthetic enzymes. *Biomedicine* 8: 352, 2020.
10. Chen H, Qi Q, Wu N, Wang Y, Feng Q, Jin R and Jiang L: Aspirin promotes RSL3-induced ferroptosis by suppressing mTOR/SREBP-1/SCD1-mediated lipogenesis in PIK3CA-mutated colorectal cancer. *Redox Biol* 55: 102426, 2022.
11. Xiao MD, J.X: Effect of reduced glutathione on high glucose-induced reactive oxygen species, nuclear factor-kappa B and osteopontin in human renal tubular epithelial cells. *Jiangsu Med J* 34: 2008.
12. Leary SLU, W.; Anthony, R.; Cartner, S.; Corey, D.; Grandin, T.; Greenacre, C.; Gwaltney-Bran, S.; McCrackin, M.; Meyer, R.; Miller, D.; Shearer, J.; Yanong, R.; Golab, G.; Patterson-Kane E AVMA guidelines for the euthanasia of animals: 2013 edition. 2013. <https://www.avma.org/KB/Policies/Pages/Euthanasia-Guidelines.aspx>
13. Meng XZ, Ni; Zhang, Min; Song, Xuexia; Liu, Qian; Huang, Xiangyan: Effect of reduced Glutathione on serum and urinary concentration of NGAL in the rodent model of Cisplatin induced acute kidney injury. *China J Modern Med* 24: 2014.
14. Livak KJ and Schmittgen TD: Analysis of relative gene expression data using real-time quantitative PCR and the 2(-Delta Delta C(T)) method. *Methods* 25: 402-408, 2001.
15. Goren O and Matot I: Perioperative acute kidney injury. *Br J Anaesth* 115 (Suppl 2): ii3-ii14, 2015.
16. Kim-Campbell N, Gretchen C, Callaway C, Felmet K, Kochanek PM, Maul T, Wearden P, Sharma M, Viegas M, Munoz R, *et al*: Cell-free plasma hemoglobin and male gender are risk factors for acute kidney injury in low risk children undergoing cardiopulmonary bypass. *Crit Care Med* 45: e1123-e1130, 2017.
17. Liu D, Zhang C, Hu M and Su K: Scutellarein relieves the death and inflammation of tubular epithelial cells in ischemic kidney injury by degradation of COX-2 protein. *Int Immunopharmacol* 101: 108193, 2021.
18. Lane D, Metselaar B, Greenough M, Bush A and Ayton S: Ferroptosis and NRF2: An emerging battlefield in the neurodegeneration of Alzheimer's disease. *Essays Biochem* 65: 925-940, 2021.
19. Xiong R, He R, Liu B, Jiang W, Wang B, Li N and Geng Q: Ferroptosis: A new promising target for lung cancer therapy. *Oxid Med Cell Longev* 2021: 8457521, 2021.
20. Li C, Sun G, Chen B, Xu L, Ye Y, He J, Bao Z, Zhao P, Miao Z, Zhao L, Hu J, You Y, Liu N, Chao H, Ji J. Nuclear receptor coactivator 4-mediated ferritinophagy contributes to cerebral ischemia-induced ferroptosis in ischemic stroke. *Pharmacol Res* 174: 105933, 2021.
21. Bao Z, Liu Y, Chen B, Miao Z, Tu Y, Li C, Chao H, Ye Y, Xu X, Sun G, *et al*: Prokineticin-2 prevents neuronal cell deaths in a model of traumatic brain injury. *Nat Commun* 12: 4220, 2021.
22. Wang J, Liu Y, Wang Y and Sun L: The cross-link between ferroptosis and kidney diseases. *Oxid Med Cell Longev* 2021: 6654887, 2021.
23. Wang Y, Quan F, Cao Q, Lin Y, Yue C, Bi R, Cui X, Yang H, Yang Y, Birnbaumer L, *et al*: Quercetin alleviates acute kidney injury by inhibiting ferroptosis. *J Adv Res* 28: 231-243, 2021.
24. Martines A, Masereeuw R, Tjalsma H, Hoenderop J, Wetzels J and Swinkels D: Iron metabolism in the pathogenesis of iron-induced kidney injury. *Nat Rev Nephrol* 9: 385-398, 2013.
25. Zhao Z, Wu J, Xu H, Zhou C, Han B, Zhu H, Hu Z, Ma Z, Ming Z, Yao Y, *et al*: XJB-5-131 inhibited ferroptosis in tubular epithelial cells after ischemia-reperfusion injury. *Cell Death Dis* 11: 629, 2020.
26. Chen C, Wang D, Yu Y, Zhao T, Min N, Wu Y, Kang L, Zhao Y, Du L, Zhang M, *et al*: Legumain promotes tubular ferroptosis by facilitating chaperone-mediated autophagy of GPX4 in AKI. *Cell Death Dis* 12: 65, 2021.
27. Vairetti M, Di Pasqua L, Cagna M, Richelmi P, Ferrigno A and Berardo C: Changes in glutathione content in liver diseases: An update. *Antioxidants (Basel)* 10: 364, 2021.
28. Santos NA, Bezerra CS, Martins NM, Curti C, Bianchi ML and Santos AC: Hydroxyl radical scavenger ameliorates cisplatin-induced nephrotoxicity by preventing oxidative stress, redox state imbalance, impairment of energetic metabolism and apoptosis in rat kidney mitochondria. *Cancer Chemother Pharmacol* 61: 145-155, 2008.
29. Han P, Qin Z, Tang J, Xu Z, Li R, Jiang X, Yang C, Xing Q, Qi X, Tang M, *et al*: RTA-408 protects kidney from ischemia-reperfusion injury in mice via activating Nrf2 and downstream GSH biosynthesis gene. *Oxid Med Cell Longev* 2017: 7612182, 2017.
30. Jia D, Zheng J, Zhou Y, Jia J, Ye X, Zhou B, Chen X, Mo Y and Wang J: Ferroptosis is involved in hyperoxic lung injury in neonatal rats. *J Inflamm Res* 14: 5393-5401, 2021.
31. Zuk A and Bonventre JV: Acute kidney injury. *Annu Rev Med* 67: 293-307, 2016.



This work is licensed under a Creative Commons Attribution-NonCommercial-NoDerivatives 4.0 International (CC BY-NC-ND 4.0) License.